Journal of Hydrology 568 (2019) 803–815

Contents lists available at ScienceDirect

Journal of Hydrology

journal homepage: www.elsevier.com/locate/jhydrol

Research papers

Climatic and hydrologic controls on net primary production in a semiarid loess watershed

Fubo Zhao[a], Yiping Wu[a,*], Bellie Sivakumar[b,c,d,e], Aihua Long[f,*], Linjing Qiu[a], Ji Chen[g], Lijing Wang[a], Shuguang Liu[h], Hongchang Hu[i]

[a] Department of Earth and Environmental Science, School of Human Settlements and Civil Engineering, Xi'an Jiaotong University, Xi'an, Shaanxi Province 710049, China
[b] School of Civil and Environmental Engineering, The University of New South Wales, Sydney, NSW 2052, Australia
[c] Department of Land, Air and Water Resources, University of California, Davis, CA 95616, USA
[d] Department of Civil Engineering, Indian Institute of Technology Bombay, Powai, Mumbai 400076, India
[e] State Key Laboratory of Hydroscience and Engineering, Tsinghua University, Beijing 100084, China
[f] State Key Laboratory of Simulation and Regulation of Water Cycle in River Basin, China Institute of Water Resources and Hydropower Research, Beijing, China
[g] Department of Civil Engineering, The University of Hong Kong, Pokfulam Road, Hong Kong, China
[h] National Engineering Laboratory for Applied Technology of Forestry & Ecology in South China, Central South University of Forestry and Technology, Changsha, Hunan, China
[i] Department of Hydraulic Engineering, Tsinghua University, Beijing, China

ARTICLE INFO

This manuscript was handled by Geoff Syme, Editor-in-Chief, with the assistance of Helge Bormann, Associate Editor

Keywords:
Biogeochemical modeling
Hydrological modeling
Net primary production
SWAT-DayCent
Water-carbon cycle

ABSTRACT

Net primary production (NPP) is one of the most important components in the carbon cycle of terrestrial ecosystems. Climatic and hydrologic elements are among the primary factors controlling the dynamics of NPP at global and regional scales. Thus, understanding the interactions between them is of great importance for optimal ecosystem management. This study aimed to investigate the spatiotemporal change in NPP and its responses to both climatic and hydrologic factors in a semiarid watershed—the Upper reach of the Wei River Basin (UWRB)—on the Loess Plateau, China. To this end, an integrated hydro-biogeochemical model (SWAT-DayCent) was applied to examine NPP during the period 1987–2016. The results show that the SWAT-DayCent performed well in simulating both the hydrologic and the biogeochemical components in this typical loess watershed. Though the basin average NPP increased slightly during the recent 30 years (1987–2016), the spatial distribution varied significantly in the region, with a relatively higher level in the southeastern and western parts and a lower level in the northern part. The strongly positive responses of major vegetations to precipitation indicate that precipitation was the dominant factor driving the ecosystem production, whereas warming may exert negative effects, especially in the southeastern part of the UWRB. Further, the strongly positive relationships between NPP and soil water/ET also suggest that the ecosystem production relied heavily on the water availability, indicating a tightly-coupled water-carbon cycle in this region. Overall, our findings are of great importance for identifying the key driving forces of the ecosystem production and the interaction between water and carbon cycles. The study may also aid policymakers in seeking better eco-environmental management when facing the climate change on the Loess Plateau.

1. Introduction

Net primary production (NPP)—the net gain in biomass by vegetation through photosynthesis—is a fundamental ecological variable in the carbon cycle of terrestrial ecosystem, because it reflects not only the production capability of vegetation but also the condition of a wide range of ecological processes (Gao et al., 2013; Li et al., 2014; Wu et al., 2014a). Spatiotemporal changes in NPP are controlled by complex factors, such as climate, land use change, and hydrologic variability (Gao et al., 2013; Pei et al., 2015; Xu et al., 2017). Among these influencing factors, the climatic and hydrologic changes are two prominent and interacting ones (McCluney et al., 2012; Zhang et al., 2014). Changes in climatic factors, particularly changes in precipitation and increasing air temperature, control the terrestrial carbon cycle mainly by regulating plant physiological processes (Liu et al., 2015; Fu et al., 2017). Hydrologic variability affects the terrestrial ecosystem

* Corresponding authors.
E-mail addresses: rocky.ypwu@gmail.com (Y. Wu), ahlong@iwhr.com (A. Long).

https://doi.org/10.1016/j.jhydrol.2018.11.031
Received 23 April 2018; Received in revised form 9 November 2018; Accepted 11 November 2018
Available online 20 November 2018

production primarily through controlling the water availability, because water is an important driver for biological processes, such as species reordering, community assembly, and biogeochemical cycling (Noy-Meir, 1973). In water-limited regions, water is the most dominant limiting resource for ecosystems because of its decisive effects on dynamics of plants and, thus, the hydrologic cycle has a profound influence on the terrestrial ecosystem production (Lohse et al., 2009; Reyer et al., 2013). Therefore, it is critical to investigate the dynamics of NPP and its dependence on climatic and hydrologic factors to achieve sustainable ecosystem management at global and regional scales.

Investigating the NPP change and its controlling factors is, however, not an easy task. Although NPP can be calculated based on some measurable variables such as tree breadth, biomass, and grain yield, such in-situ measurements and subsequent calculations are limited to small scale (e.g., plot scale or field scale) and time-consuming (Lauenroth et al., 2006). Remote sensing-based approaches can estimate NPP variations and spatial patterns, but it can hardly analyze complicated ecosystem processes and underlying internal control mechanisms and thus cannot quantify the responses of the NPP to various environmental factors (Zhang and Ren, 2017). Ecosystem models are important tools that can be used to compute NPP and associated control mechanisms at site, regional or global scales (Gao et al., 2013; Gu et al., 2017; Wang et al., 2017b). Popular models such as Carnegie-Ames-Stanford Approach (CASA) (Potter et al., 1993), CENTURY (Parton et al., 1994), and BioGeochemical Cycle (BGC) (Running and Coughlan, 1988) usually have been applied to analyze the climatic controls on NPP (Gao et al., 2013; Li et al., 2014; Liu et al., 2015; Wang et al., 2017b). As we understand, the NPP cannot be decided by a single factor, other terms such as the hydrologic cycles would play an important role in controlling the spatiotemporal patterns of NPP, which has not been investigated due to model deficiencies in handling both biogeochemical and hydrologic processes (Gramig et al., 2013). Based on Soil and Water Assessment Tool (SWAT) (Arnold et al., 1998), Wu et al. (2016) developed an integrated hydro-biogeochemical model by embedding the DayCent model into SWAT—SWAT-DayCent. The model can simultaneously simulate hydrologic and biogeochemical cycles at the watershed scale and thus can overcome the defects of traditional hydrologic/biogeochemical models that focused on either water or carbon cycle. Thus, it could be encouraging to investigate the water and carbon cycles and their interactions using SWAT-DayCent. Actually, our motivation was to investigate the spatiotemporal change in NPP and its responses to both climatic and hydrologic factors in a semi-arid loess watershed, the Wei River Basin, on the Chinese Loess Plateau.

The Wei River Basin, located in the south of the Loess Plateau region, is a typical watershed that is characterized by loess hills and gullies and severe soil erosion (Wang et al., 2017a). To restore the ecological environment and prevent soil from erosion, the Chinese government has implemented a series of engineering measures including forestation, planting of grass, and terraces at a large scale since the 1980s (Zuo et al., 2014; Wang et al., 2017a). As expected, these measures have significantly increased the vegetation cover and reduced the soil erosion, but the eco-environment in most areas of the basin is still vulnerable due to the loosened land surface and changing environments. Particularly, the newly-planted vegetations would consume more water compared to the original ones, which may complicate the relationships between the water and carbon cycles and exacerbate conflicting demands for water between plants and humans in such semi-arid area (Feng et al., 2016). So far, it has been acknowledged that the implemented ecological restoration measures changed the regional carbon cycle and its interactions with the environmental factors (Sun et al., 2014; Zhang et al., 2016a). In addition, although there is convincing evidence as to the impacts of climate change, there still exist large uncertainties (e.g., increasing temperature, change in precipitation, and extreme climate events), which can exert uncertain influences on the terrestrial carbon cycle. In this sense, it is necessary to investigate the carbon cycle and its responses to the controlling factors to enhance the understanding of the water-carbon interactions in this ecologically vulnerable region, especially in the context of climate change.

The overall goal of this study was to investigate the spatiotemporal distribution of NPP and its responses to climatic and hydrologic factors (precipitation, air temperature, soil water, and ET) in the Upper reach of the Wei River Basin (UWRB) using SWAT-DayCent. The specific objectives were to: (1) examine the applicability of the SWAT-DayCent model in simulating the water and carbon dynamics in the UWRB, (2) investigate the spatiotemporal variations of the NPP and climatic and hydrologic components, (3) explore the responses of NPP to both climatic and hydrologic variability on annual scale of all Hydrologic Response Units (HRUs) that are defined by SWAT over the 30-year study period (1987–2016). The outcomes could contribute to both the applicability of SWAT-DayCent and the understanding of interactions between water and carbon in such semi-arid loess watershed.

2. Materials and methods

2.1. Study area

The Wei River is the largest tributary of the Yellow River, and originates in the Niaoshu Mountain and flows through Gansu and Shaanxi provinces with a length of 818 km. In this study, we focused on the UWRB, i.e. the region above the Linjiacun gaging station (104°E–107°E, 34.2°N–36.2°N, 30,540 km^2) (Fig. 1). The UWRB lies in the continental monsoon climate zoon, with relatively more precipitation and high temperature in summer and less precipitation and low temperature in winter. The annual precipitation ranges from 500 to 800 mm and the annual mean temperature ranges between 7.8 and 13.5 °C (Liu et al., 2012; Zhao et al., 2016). Topographically, the altitude decreases from the highest northwestern mountain areas to the lowest southeastern plain areas.

2.2. Land use and soil types

The land use and soil types were obtained from the Ecological and Environmental Science Data Center for West China (http://westdc.westgis.ac.cn) with a resolution of 30 m × 30 m and 1 km × 1 km, respectively, and the details are shown in Fig. 2. The land use types were divided into 7 types and a further 10 subtypes. The seven types mainly include forest, grassland, cropland, shrubland, residential area, water, and bare land. As shown in Fig. 2, the forest type includes forest mixed (FRST), forest deciduous (FRSD), and forest evergreen (FRSE); the grassland includes pasture (PAST) and range grasses (RNGE); the cropland means agricultural land (AGRR); shrubland means the range brush (RNGB); the residential area means URBN; water means water bodies (WATR); and the bare land is BARR. Cropland is the major land use type, accounting for 66%, and continuous wheat or maize and corn-wheat rotation are the most common cropping systems in the region. As seen from Fig. 2, there are 27 groups of soil types and the Cambisols is the dominant one, accounting for 50% of the area.

2.3. SWAT-DayCent coupler

To achieve a comprehensive evaluation of environmental issues, Wu et al. (2016) developed a model coupling tool (SWAT-DayCent) for simultaneous hydro-biogeochemical modeling using SWAT (Soil and Water Assessment Tool) (Arnold et al., 1998; Neitsch et al., 2011) and DayCent (Parton et al., 1998). The SWAT model, developed by the U.S. Department of Agriculture (USDA) Agricultural Research Service (ARS), is a watershed-scale, continuous, distributed hydrologic model for predicting the impacts of climate and land management practices on hydrologic and water quality at the watershed scale (Arnold et al., 1998; Neitsch et al., 2011). This physically-based model has been increasingly applied to study the impacts of environmental change on

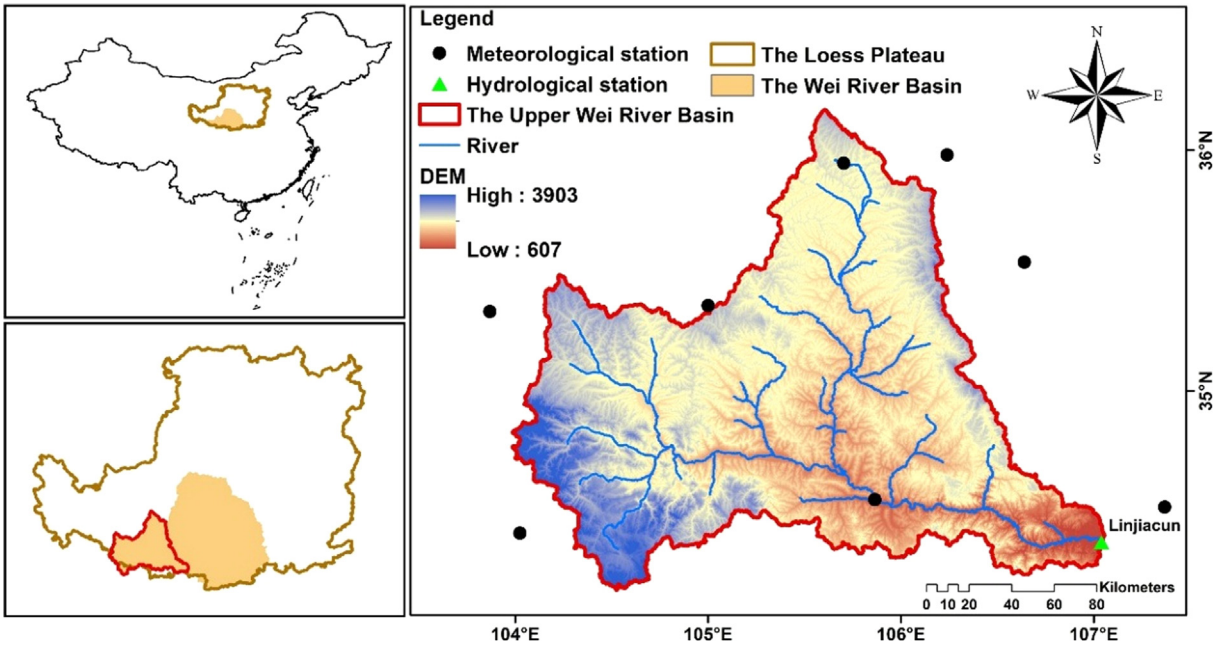

Fig. 1. Location and elevation of the Upper Wei River Basin above Linjiacun.

hydrologic cycle in many large watersheds, including those with limited observations (Arnold et al., 2000; Neitsch et al., 2011; Panagopoulos et al., 2015). DayCent is the daily time version of CENTURY—a biogeochemical model that simulates major processes associated with flows and cycling of carbon (C), nitrogen (N), phosphorus (P), and sulfur (S) among the atmosphere, vegetation, and soil pools at the site scale (Parton et al., 1998; Del Grosso et al., 2006). DayCent has been proven to be capable of simulating the carbon dynamics with a high accuracy (Del Grosso et al., 2006). In the coupling of SWAT and DayCent, the SWAT was set as the basic framework and the DayCent was embedded into SWAT with some new functions, whose aim is to take each HRU as a single site and write DayCent required input files to drive DayCent automatically. The HRU is generated in the SWAT running process and its configuration is required for the DayCent simulation. Each HRU has the unique soil and land cover type, and can be used as a specific site in DayCent. DayCent then obtains the specific variables in HRU to simulate the carbon cycle across all HRUs through a loop. In the coupling simulation processes, the hydrologic cycle is simulated by SWAT and the biogeochemical cycle is mainly dependent on DayCent (see Table 2). Major outputs of SWAT-DayCent include the hydrologic components (e.g., surface runoff, baseflow, ET, soil water, and water yield) and the biogeochemical components (e.g., NPP, soil organic carbon (SOC), biomass, grain yield, and soil respiration). Further details about SWAT-DayCent can be found in Wu et al. (2016).

2.4. Model input and setup

Besides the land use (30 m × 30 m) and soil type (1 km × 1 km) data, the SWAT model also requires inputs on weather and topography data (Arnold et al., 2000). The daily meteorological data were collected from the Data Center of China Meteorological Administration (http://data.cma.cn), covering the study period during 1987 to 2016, consisting of precipitation, maximum/minimum air temperature, relative humidity, and wind speed. The solar radiation was derived based on the sunshine duration. The Digital Elevation Model (DEM) was from the Shuttle Radar Topography Mission (SRTM) with a 90-m resolution (Jarvis et al., 2006). The land use and soil data were obtained from the Ecological and Environmental Science Data Center for West China (http://westdc.westgis.ac.cn). The Geographic Information System (GIS) interface, ArcSWAT (version 2012), was used to delineate the watershed, resulting in 95 sub-basins and 2605 HRUs.

The monthly streamflow data of Linjiacun hydrologic station (see Fig. 1), obtained from the Hydrological Yearbooks of Yellow River, were used to calibrate/validate the SWAT model. The remotely-sensed NPP data were used for the DayCent calibration/validation. We collected the NPP data from two sources: one was the MODIS Net Primary Production Yearly L4 Global 1-km products (MODIS17A3, https://lpdaac.usgs.gov); the other was from the Resources and Environment Science Data Center of the Chinese Academy of Sciences (RESDC, http://www.resdc.cn). Considering the complexity of the ecosystems and the data reliability, we compared these two data products with previous literature (Feng et al., 2013; Peng et al., 2015; Zhang et al., 2016a; Wei et al., 2017), including the specific NPP value in each land cover type. We found that the cropland-NPP produced by MODIS was acceptable for our study region and that the grassland-NPP and forest-NPP produced by RESDC were also relatively reasonable. Therefore, we combined these two datasets for the DayCent verification.

2.5. Model calibration and validation

Both SWAT and DayCent contain parameters that need to be determined for a specific region through comparison with the observed data. For SWAT, based on previous publications (Wu et al., 2012; Wang et al., 2017a; Yan et al., 2017; Zhao et al., 2018b) and our own experience, we selected eight parameters that are sensitive to runoff simulation. We implemented the calibration and validation by using the daily and monthly observed streamflow from 1973 to 1993. The calibrated parameters are listed in Table 1.

For DayCent, based on the literature review (Wu et al., 2014b; Wu et al., 2014c; Rafiqu et al., 2015; Qiu et al., 2017) and our own modeling experience, we selected the most sensitive parameter “PRDX”. We used the Model-R Coupler (Wu et al., 2014d) to derive the optimal parameter value by comparing the simulated NPP with the remotely-sensed NPP that were available for 11 years (2000–2010) and the optimized “PRDX” parameter for forest, crop and grass is 8.6, 0.42, and 0.48 $g\,C\,m^{-2}\,month^{-1}$ $Langley^{-1}$, respectively.

The model performance was mainly evaluated in terms of the Nash-Sutcliffe Efficiency (NSE) (Nash and Sutcliffe, 1970), r^2, Percentage Bias (PB), and Root Mean Square Error (RMSE). A brief description of these measures is presented in Appendix A.

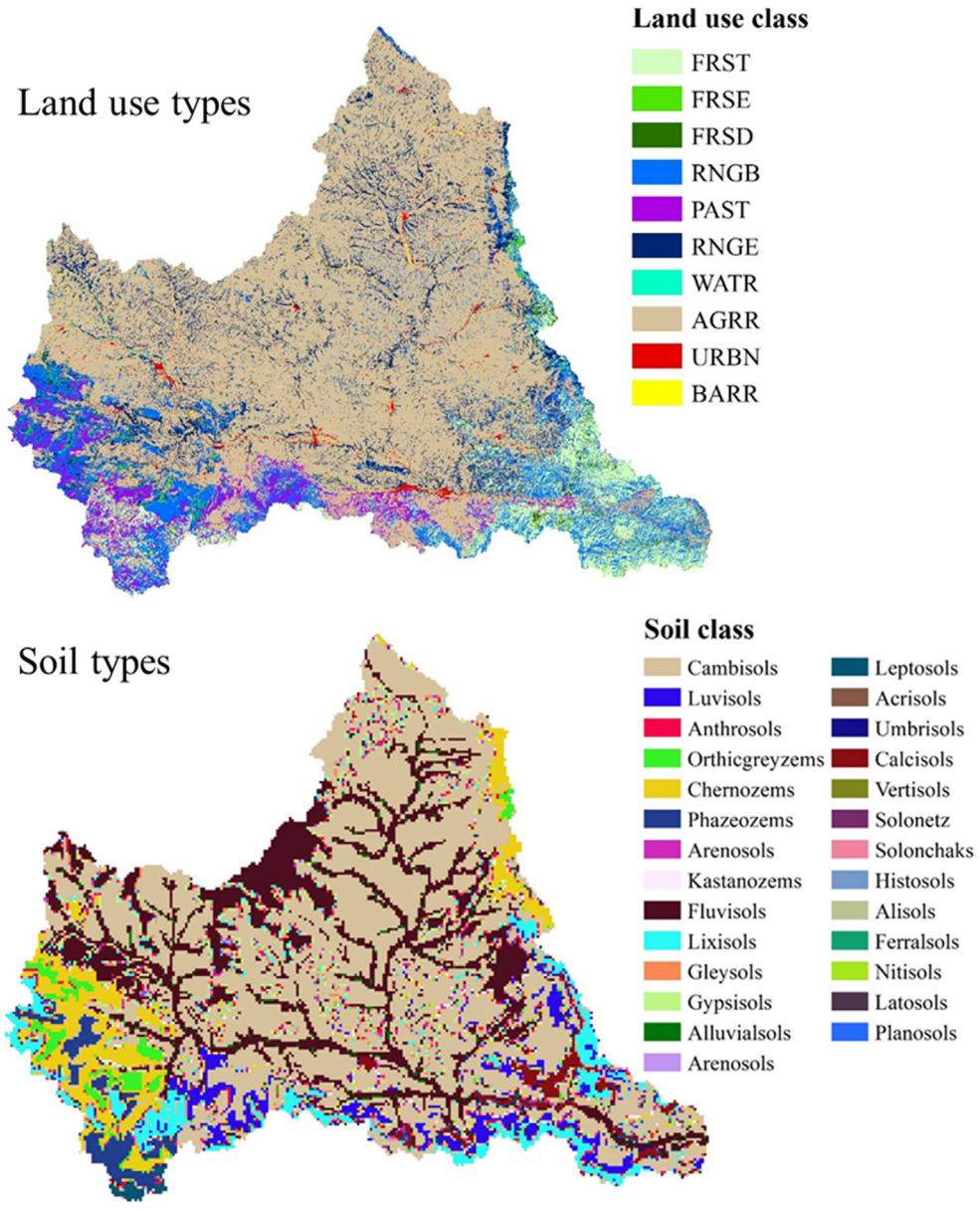

Fig. 2. Land use and soil types in the Upper Wei River Basin. FRST: forest-mixed, FRSE: forest-evergreen, FRSD: forest-deciduous, RNGB: range brush, PAST: pasture, RNGE: range grasses, WATR: water body, AGRR: agriculture land, URBN: urban, BARR: bare land.

Table 1
SWAT Calibrated parameters for the Upper Reach of the Wei River Basin.

Parameters	Description	Range	Calibration result
CN2	Curve number II value	−0.2–0.2	0.1*
ALPHA_BF	Baseflow recession factor	0.001–1.0	0.005
ESCO	Soil evaporation compensation factor	0.001–1.0	0.5
SOL_AWC	Soil available water capacity	0.0–1.0	0.26*
SOL_K	Saturated hydraulic conductivity (mm h^{-1})	−0.2–0.2	−0.15*
CH_K2	Effective hydraulic conductivity in main channel	0.0–20.0	2.5
SLSUBBAN	Average slope length (m)	−1.0–1.5	0.8*
HRU_SLP	Average slope steepness (m m^{-1})	−1.0–1.5	1.2*

* Relative change: the existing parameter value is multiplied by (1 + given value).

2.6. Trend and correlation analyses

We used the least square method to obtain the linear fitting lines and trends in NPP at the HRU level. The equation for calculation of slope is presented in Appendix B. The *t*-test was applied to determine the significant levels ($P < 0.05$) of the trends in NPP.

To analyze the relationships of NPP with soil water and ET, we employed the simple linear regression model and calculated the Pearson correlation coefficients at the HRU level over the study period of 30 years. To establish the relationships of NPP with precipitation and temperature, the partial correlation analysis was used to detect whether one climatic element (i.e., precipitation/temperature) affects NPP variability independent of the other (i.e., temperature/precipitation). The equations for calculation of these are presented in Appendix C.

Table 2
Processes simulated by SWAT and DayCent.

Model	Process
SWAT	Hydrologic cycle (e.g., surface runoff, ET, soil water movement, overland flow, baseflow, lateral flow, infiltration, percolation)
DayCent	Biogeochemical cycle (e.g., plant growth, NPP, carbon allocation, soil organic carbon pool and dynamics, soil respiration, and nitrogen emission (N_2O mission))

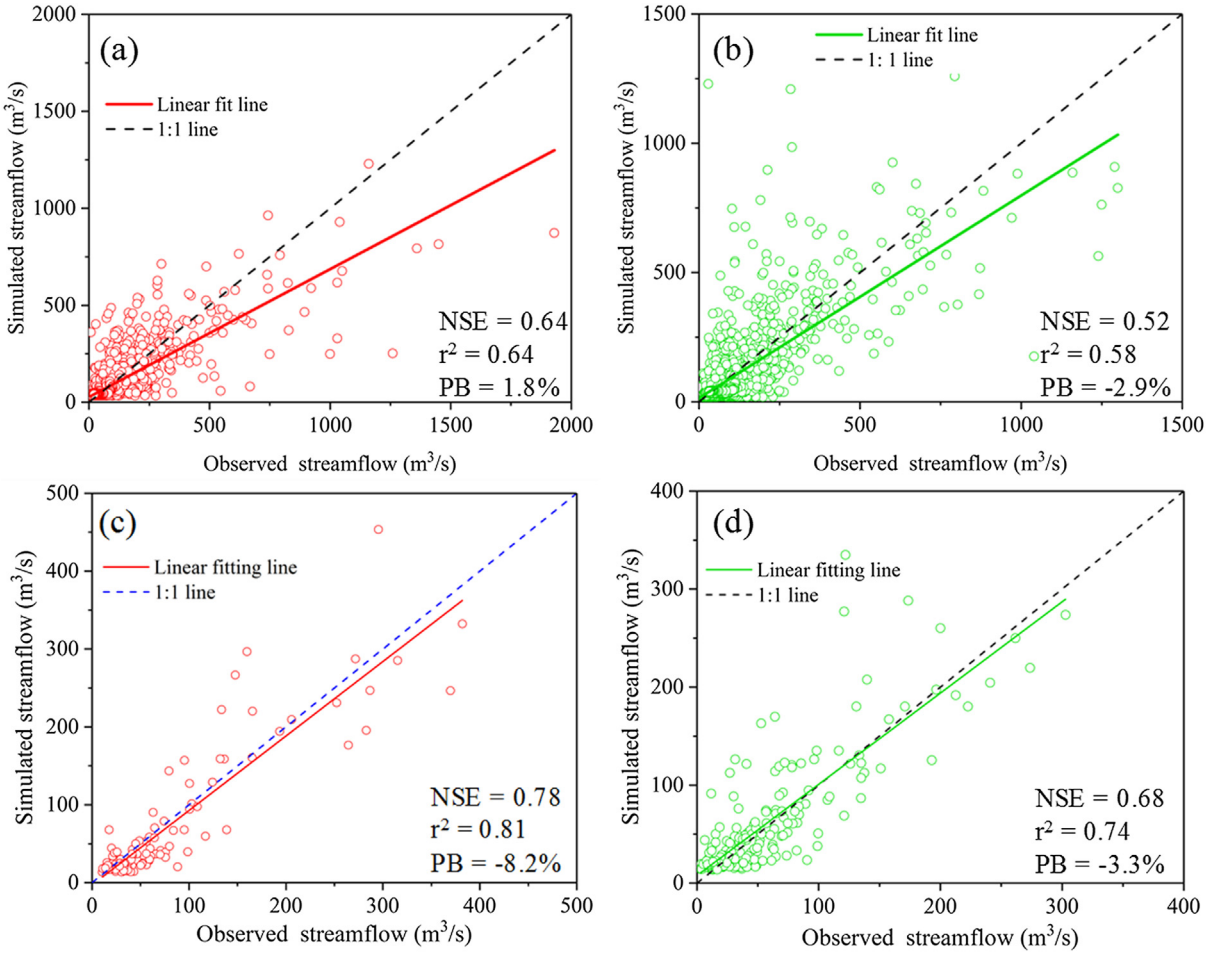

Fig. 3. Model performance for the (a) daily 8-year calibration (1973–1980) and (b) 12-year validation (1981–1993) and the (c) monthly 8-year calibration and (d) 12-year validation.

3. Results

3.1. Model examination

Fig. 3 shows the scatterplots and the evaluation measures for both the daily and monthly streamflow simulation in the 8-year calibration and the 12-year validation period. For the daily simulation, the model performed well in the calibration period (1973–1980), with NSE, r^2, and PB values of 0.64, 0.64, and 1.8%, respectively. In the 12-year (1981–1993) validation period, the model performance was satisfactory, though the criteria (with NSE, r^2 and PB values of 0.52, 0.58 and -2.9%) were not as good as those in calibration. For the monthly simulation, the simulated streamflow matched well with the observations. From Fig. 3c and Fig. 3d and according to Moriasi et al. (2007), who reported that the model performance should be 'very good' when NSE > 0.75 and |PB| < 10% and 'good' when NSE > 0.65 and |PB| < 10%, the model performance can be rated as 'very good' in calibration and 'good' in validation for the monthly simulation. Overall, the SWAT model performance was acceptable for simulating the hydrological processes in the UWRB.

Fig. 4 shows the scatterplots of the annual NPP simulations for the period 2000–2010, for the three major land cover types (i.e. forest, cropland, and grassland) as well as the total ecosystem. The statistical evaluation measures (also presented in Fig. 4) illustrate that the |PB| were less than 2%, r^2 ranged from 0.36 to 0.63, and the RMSE varied from 19.1 to 41.8 g C/m^2/yr, considering all the above four cases (i.e. three land cover types and the total ecosystem), indicating the DayCent simulated NPP with very small bias and high precision. Therefore, the DayCent can also be applicable in the UWRB.

3.2. Inter-annual variations of NPP and controlling factors

Fig. 5 shows the inter-annual variations of NPP and its four controlling factors considered in this study (i.e. precipitation, air temperature, ET, and soil water), for the period 1987–2016. The mean annual NPP was 311 g C/m^2/yr, with a range from 213 g C/m^2/yr in 1997 to 352 g C/m^2/yr in 2012 (see Fig. 5a). Although the NPP changed, sometimes significantly, between years during the 30-year period, it showed only a slightly increasing trend at a rate of 0.69 g C/m^2/yr, which was not statistically significant. The annual air

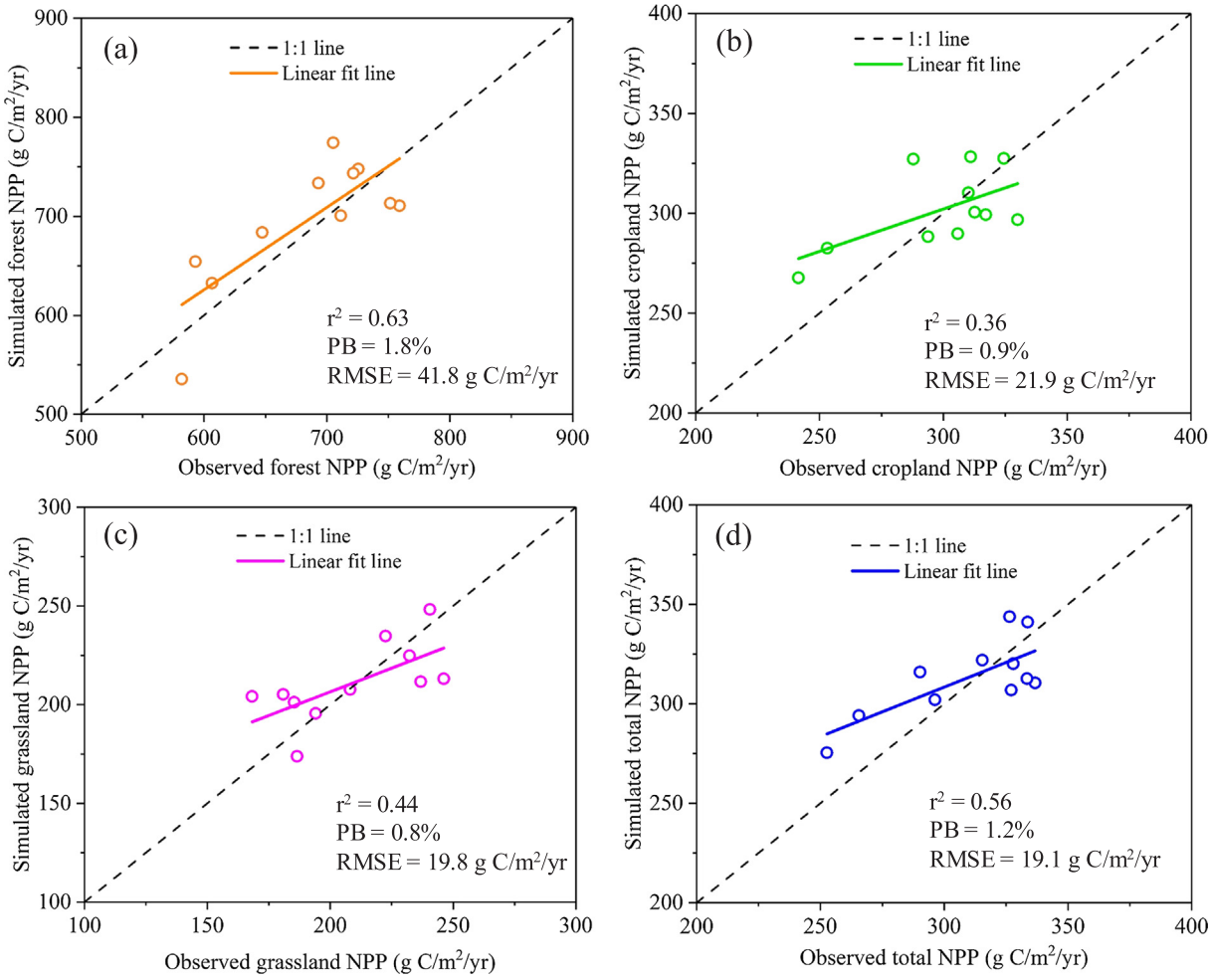

Fig. 4. Comparison of annual NPP of the UWRB from the DayCent-simulated and remotely-sensed NPP for three major land cover types: (a) Forest, (b) Cropland, (c) Grassland, and the (d) whole basin.

temperature showed a significant rising trend of 0.04 °C/yr ($P < 0.001$) with an average of 9.1 °C and a range of 8.1–10.3 °C. The overall trend of the precipitation was relatively stable, especially when compared with the air temperature, though the fluctuation was obvious among years (Fig. 5a). Particularly, we can see that the trends of NPP generally matched the temporal variation of precipitation. The ET showed a very slight tendency during the whole study period, with the highest value (560 mm) in 1990 and the lowest value (336 mm) in 1997 across the whole study period (Fig. 5b). The soil water content increased slightly over the whole study period with some significant changes during 2002–2004, an increase of 97 mm from 2002 to 2003, followed by a reduction of 72 mm from 2003 to 2004.

3.3. Spatial pattern and changing trend of NPP

Fig. 6 shows the distributions of the average annual NPP and its changing trend in UWRB during the period 1987–2016. Overall, the NPP exhibited large spatial variability with a gradually decreasing trend moving from the south to the north across the region. Specifically, higher NPP was found in the western and southeastern parts of the region, whereas lower NPP was in the northern and northeastern parts (Fig. 6a). The areas where the NPP had a significant increasing trend were mainly distributed in the central north and some parts of the northwestern and southeastern areas, while the decrease in NPP was mainly distributed in the central south and northeastern portion (Fig. 6b). Among the major land cover types, the increases in NPP were larger in cropland and grassland (Fig. 6c), accounting for as high as 92% of the areas contributing to an increased NPP. In contrast, the forest had a relatively larger area (65%) of decreased NPP (Fig. 6c).

3.4. Response of NPP to climatic factors

The spatiotemporal partial correlation coefficients of NPP with the two climatic factors (precipitation and air temperature), calculated for each HRU from 1987 to 2016, are shown in Fig. 7. Spatially, the correlation coefficients between NPP and precipitation were all positive with a significant level ($P < 0.05$) (Fig. 7a). Fig. 7b indicates that the partial correlations between NPP and precipitation among HRUs were also generally positive with the value being larger than 0.4 for most areas, suggesting strong control from precipitation on the regional NPP dynamics. The average value of the coefficient was positive in all the three major land cover types (see the inserted boxplot in Fig. 7b). As seen from Fig. 7c, there existed negative and insignificant relationships between NPP and temperature in space, indicating higher temperature may generate adverse effects on plant production in some areas of this region. In addition, there was also a relatively larger variation of the partial correlation between NPP and air temperature (Fig. 7d). The negative correlations were mainly found in the southeastern part and some areas of the northeastern and far northwestern region, while the positive correlation was mainly found in the southwestern part and central to northern part. The average value of the coefficient was positive in the forest, whereas the values for cropland and grassland were negative (see the boxplot in Fig. 7d). This indicates that warming may exert negative effects on the NPP of the local ecosystems, especially in

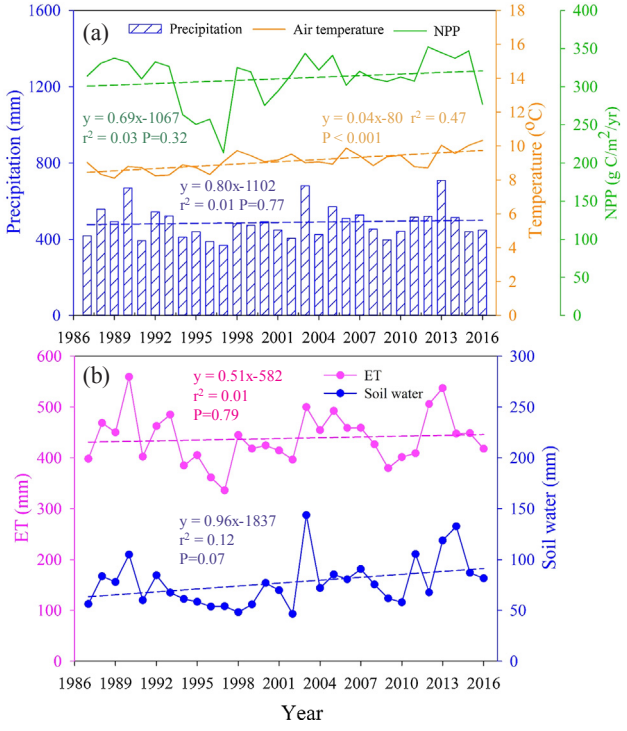

Fig. 5. Inter-annual variations in NPP and climatic and hydrologic variables in the UWRB during the past 30 years (1987–2016): (a) NPP, precipitation, temperature; (b) ET, and soil water.

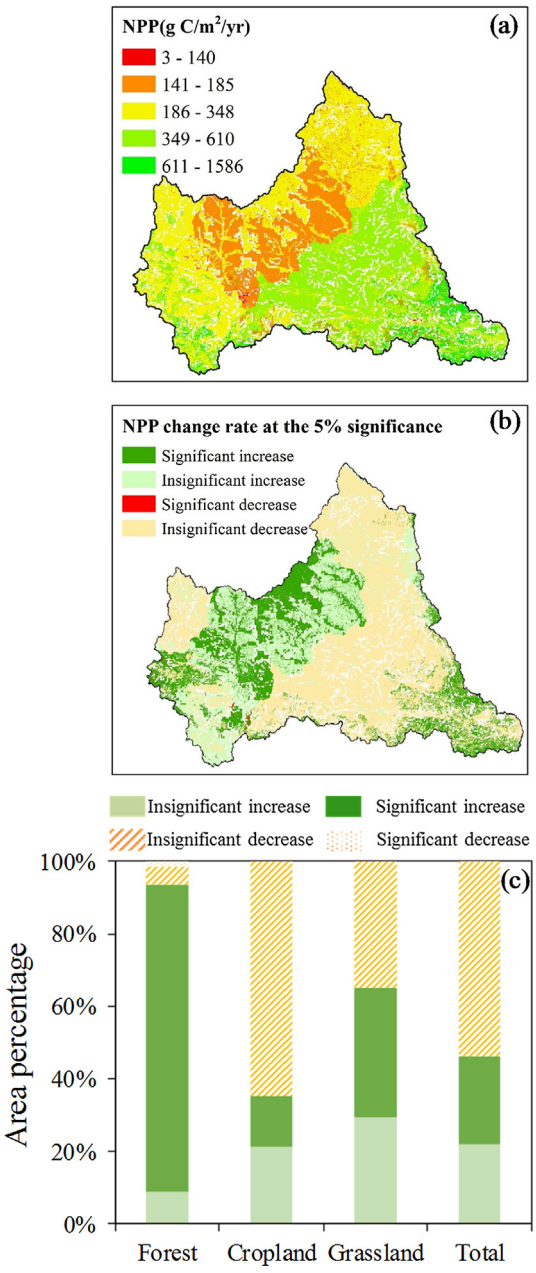

Fig. 6. (a) Spatial patterns of average annual NPP over the period 1987–2016; (b) spatial distribution of trends of annual NPP with a statistically significant test at the 5% confidence level; and (c) the area proportion of NPP change in the UWRB.

the southeastern part of the basin.

3.5. Response of NPP to hydrologic factors

Fig. 8 shows the linear relationships of NPP with soil water and ET for the three major land cover types over the period 1987–2016, together with the distribution of Pearson correlation coefficients between them at the HRU level. As seen, the NPP in grassland and cropland were significantly positive with the soil water ($P < 0.05$), while the forest showed no significant relationship with soil water (Fig. 8a). As can be seen from Fig. 8b, most areas of this region showed positive correlation between NPP and soil water, indicating that the ecosystem production relied heavily on the soil water. The annual NPP was also positively correlated with the annual ET for the three major land covers ($P < 0.001$) (Fig. 8c). From Fig. 8d, it can be seen that the northeastern and western parts had stronger positive correlations between NPP and ET compared with that in the other parts. The strong relationship between NPP and ET suggests that the water and carbon cycles in this region were tightly coupled.

4. Discussion

4.1. Uncertainty in SWAT-DayCent simulations

Uncertainty in model simulations, which is mainly caused by the limitations of model parameters and algorithms, is a major challenge in analyzing modeling results. In our study, the SWAT model performed well in both simulating the daily and monthly streamflow, with NSE ranging from 0.52 to 0.78 and r^2 ranging from 0.58 to 0.81. However, the model also overestimated some peak flows (not shown) and the possible reasons may be the coarse resolution of rainfall and/or the limitations of the model in catching the hydrologic response to high intensity of rainfall (Zhou et al., 2011). Besides, the observed streamflow was the only variable used to calibrate and validate the SWAT model in our study, which may also lead to uncertainties in other output elements. No matter how well a model is calibrated using one specific variable, the other model outputs such as ET, soil water, and water yield might have a certain bias due to the lack of accurate identification of the key parameters related to their simulation. Calibrating the SWAT model using multiple variables (e.g., ET, soil water, and lateral flow) can be an effective way to reduce the uncertainty. As more variables related to water balance such as the remote-sensing ET and remote-sensing soil moisture have been becoming available, the multi-variable calibration would be an important step towards reducing the uncertainty in SWAT and other land surface models in the future research. Another source leading to uncertainty in SWAT simulations is the size of the target region/basin. Qiao et al. (2015) reported that the SWAT model performed much better in a relatively small watershed than that in a larger one, because the meteorological data could not accurately represent the spatial heterogeneity in the chosen parameters

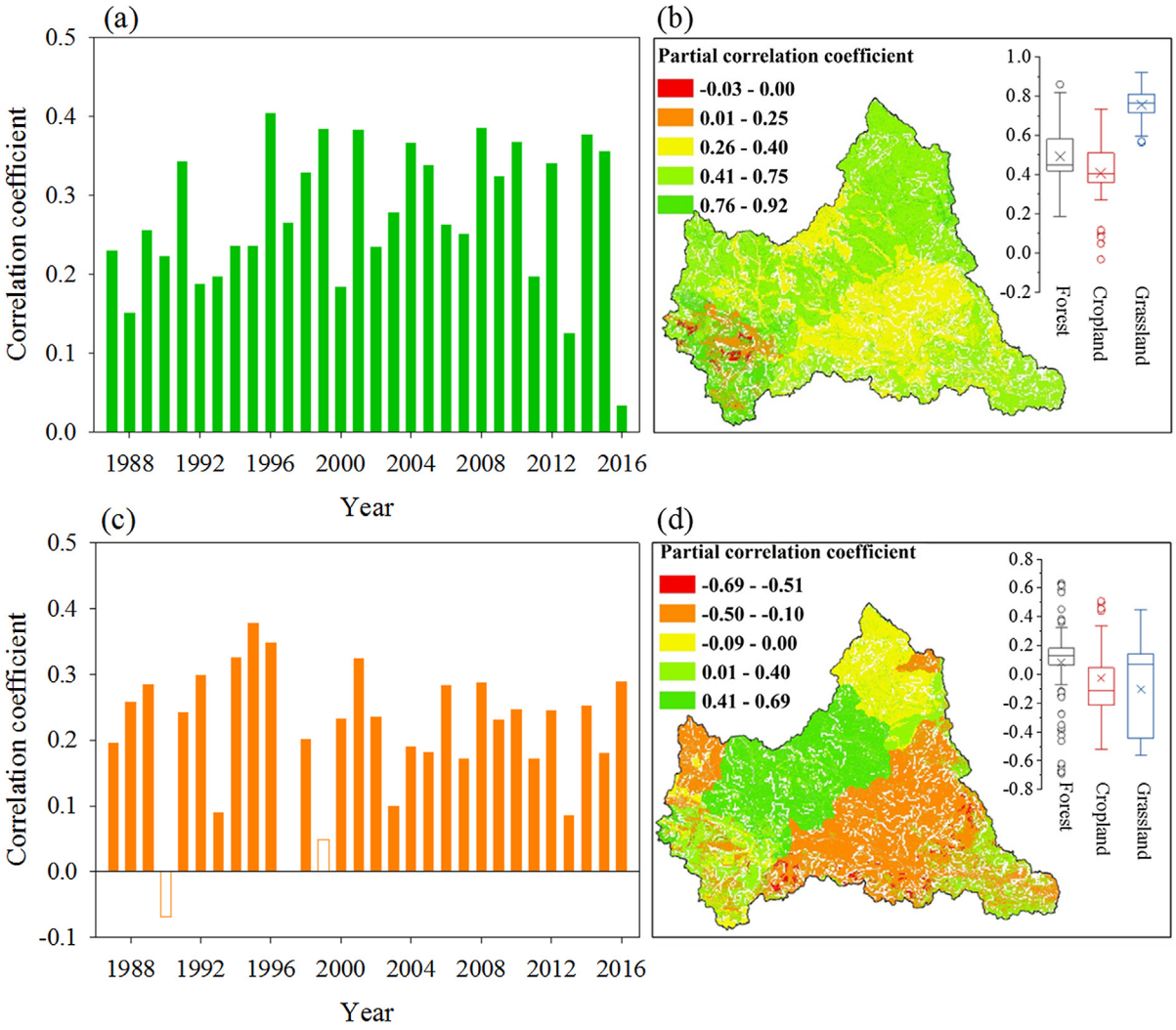

Fig. 7. Spatiotemporal partial correlation between NPP and climate. (a) spatial partial correlation coefficient between NPP and precipitation in each year, (b) distribution of temporal partial correlation coefficient between NPP and precipitation, (c) partial correlation coefficient between NPP and air temperature in each year, (d) distribution of temporal partial correlation coefficient between NPP and air temperature. A filled green or orange bar indicates significant correlation coefficient between precipitation or air temperature and NPP ($P < 0.05$), and an unfilled bar indicates no significant correlation exists. The cross and solid lines in the boxplot mean the average and median value of the partial correlation coefficient, respectively. (For interpretation of the references to color in this figure legend, the reader is referred to the web version of this article.)

over large basins. While the area of UWRB, considered in our study, exceeds 30,000 km^2, only eight meteorological stations were available. This may have contributed to bias in streamflow simulation.

It is important to recognize that, compared with hydrologic modeling, it is more difficult to simulate NPP. On the one hand, as a site-scale model, the simulation of DayCent should be better in the spot simulation when compared to the one that scales up for large areas and long-time scale due to the spatial heterogeneity of data. On the other hand, although the remote sensing techniques can reflect the features of the NPP at regional scale, it can also predict NPP with bias due to multiple influencing factors (e.g., meteorological conditions, topography, sensors) (Zhao et al., 2005; Zhao et al., 2006). Moreover, the NPP measurement in reality is also difficult, because it is hard to partition the respiration of ecosystems into autotrophic and heterotrophic respiration (Gao et al., 2013). In our study, we combined two remote sensing NPP products, and the comparison between the simulated and remotely-sensed NPP indeed indicated that the DayCent simulation was acceptable.

4.2. Spatiotemporal change of NPP

The NPP showed obvious spatial variability, with higher NPP in the southeastern and western parts but lower NPP in the northern part across the UWRB region (Fig. 6a). This distribution is consistent with the vegetation cover as well as the rainfall distribution. For example, the cropland and productive forest were densely distributed in the southeastern and western areas, leading to higher NPP in those regions. From Fig. 6a&b, the areas with higher NPP tended to decrease over the study period, while the areas with lower NPP showed an increasing tendency. This phenomenon may suggest that the carbon uptake in this region tended to be balanced spatially. Our analysis of the 30-year simulation revealed an overall increasing rate of 0.69 g $C/m^2/yr$ in the UWRB (Fig. 5a). However, this estimated increasing rate is less than the estimated increasing rate (9.4 g $C/m^2/yr$) over the whole Loess Plateau region from 2000 to 2008 (Feng et al., 2013). This discrepancy can be mainly explained by the difference in study period and area. Our results were also consistent with the finding, by a number of studies (Su and Fu, 2013; Wang et al., 2013; Liu et al., 2015), that the terrestrial vegetation NPP of the Loess Plateau region has increased during the past several decades, suggesting the potential carbon gain in this region.

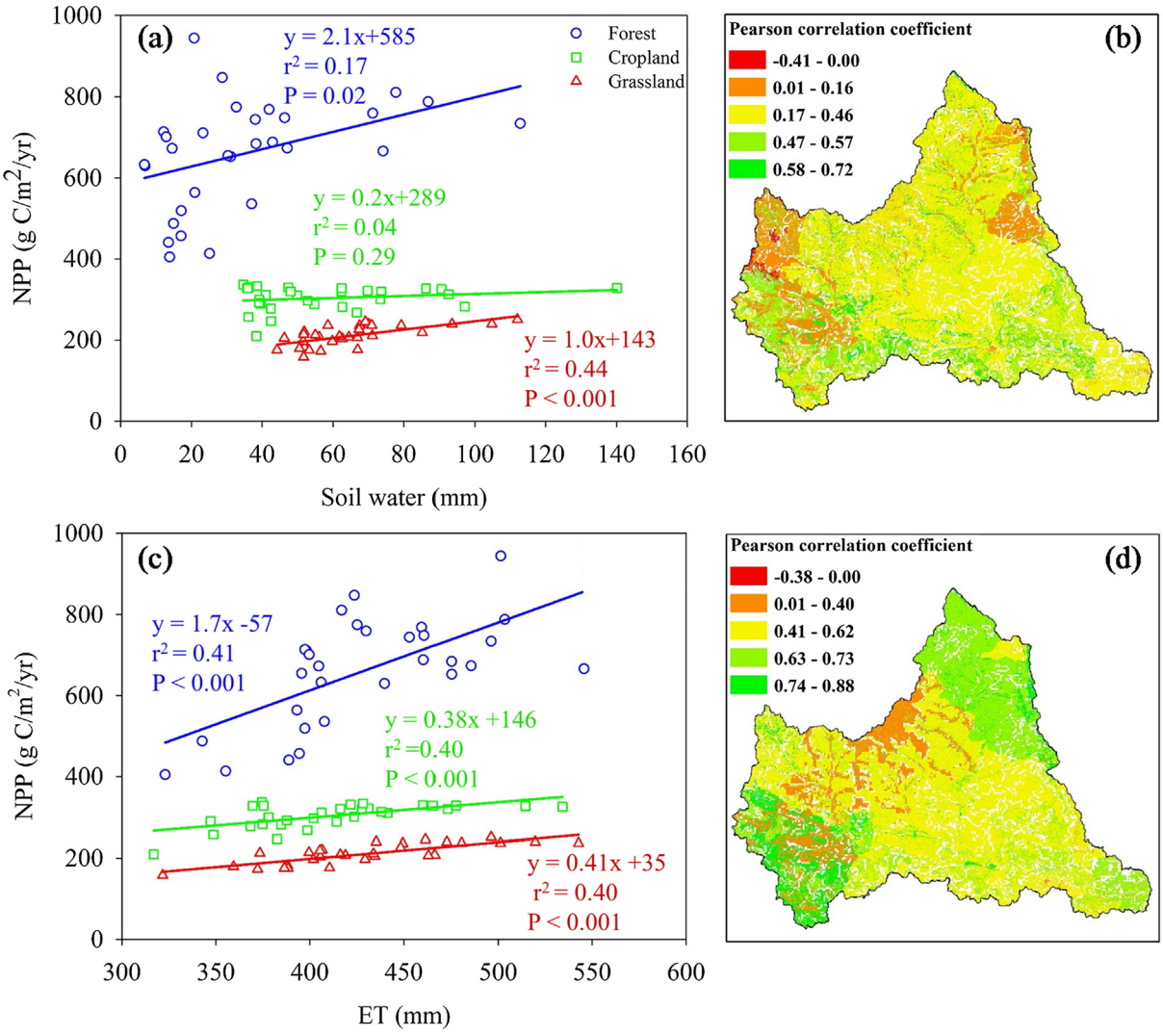

Fig. 8. (a) Relationship between NPP and soil water during the past 30 years; (b) the spatial distribution of Pearson coefficient between NPP and soil water; (c) relationship between NPP and ET during the last 30 years; and (d) the spatial distribution of Pearson correlation coefficient between NPP and ET.

4.3. Climatic and hydrologic controls on NPP

In most areas of the UWRB region, the NPP displayed a positive correlation with precipitation (Fig. 7a), suggesting that the precipitation is the dominant factor driving the vegetation growth in this region. The Loess Plateau region is becoming warmer and drier (Xin et al., 2010). Since precipitation is the only water supply for the 'rain-fed' ecosystems of the region, the vegetation growth depends heavily on the precipitation. However, the areas where NPP was positively correlated with temperature accounted for only 44% of the whole basin. Traditionally, high temperature can stimulate the vegetation growth. However, the temperature control on NPP is mainly distributed in the humid and semi-humid region where the water availability is not a limiting factor for vegetation growth (Liang et al., 2015). High temperature and combined rainfall deficit can reduce plant production to some extent (Ciais et al., 2005; Huang et al., 2017), especially in the water-deficient regions. Interestingly, the air temperature increased significantly ($P < 0.001$), together with a slight increase in NPP, while more than fifty percent of the area negatively correlated with the temperature (Fig. 7b). This indicates that the positive effect of precipitation offset, at least partly, the negative effect of temperature, demonstrating the key role of precipitation in the ecosystem production of this region.

We also found that NPP in the three major land cover types was positively correlated with soil water and ET, which is also supported by other reports (French et al., 2009; Lima et al., 2013; Chen et al., 2016; Tang et al., 2016; Zhao et al., 2018a). Soil water is a crucial factor determining the production, because higher soil moisture content will lead to higher photosynthesis through controlling the stomatal morphology and, thus, higher production (Liu et al., 2013). The strong correlation between NPP and soil water suggested that the carbon gain depends heavily on the water availability in this region. However, the soil in the Loess Plateau is drying due to the widespread overplanting (Zhang et al., 2018), suggesting that the vegetation production might be suppressed under the drier condition. This phenomenon may alert the managers to make more efficient measures when implementing the revegetation to maintain a sustainable ecohydrological environment in this region. The plant growth rate and transpiration are usually tightly related to each other (Vicente-Serrano et al., 2015; Barkaoui et al., 2017), and higher ET usually reflects higher plant transpiration, indicating stronger plant canopies and, thus, higher plant production. The strong correlation between NPP and ET demonstrated that carbon and water cycles were tightly linked in this region, and thus the magnitude of ET can reflect the ecosystem healthy condition. In fact, the slope of the relationship between NPP and ET can also be an indicator for evaluating water use efficiency and ecosystem services in a certain ecosystem. In addition, the strong positive relationship between ET and NPP implied that higher ET corresponded to a higher carbon uptake of NPP, which may help estimate NPP using ET.

Table 3
Comparison of the study findings with globe-wide studies.

Region	Period	NPP trend (gC/m^2/yr)	Response to climatic and hydrologic components (correlation coefficient)				Methods	References
			Pre	Tem	SW	ET		
Central Aisa	1980–2014	−0.82	0.83**	−0.41*	–	–	AEM model	Zhang and Ren (2017)
China	1982–2010	Grassland:0.88** Cropland:1.85**	0.09	> 0.5**	–	–	CASA model	Liang et al. (2015)
TRSR	1982–2012	1.31	0.58	0.73	–	–	CASA model	Zhang et al. (2016b)
Tibetan Plateau	2000–2008	–	−0.61	0.91	–	–	LUE model	Gao et al. (2013)
Inner Mongolia Steppe Grasses	1955–2010	–	0.98††	–	–	1.00††	SPAW model	Wang et al. (2014)
Arizona	2003–2007	–	0.91**	–	–	0.62*	In-situ measure	Scott et al. (2014), (2015)
North America	2000–2012	–	–	–	–	U.S.:0.65* Canada:0.62*	Flux observation	Xiao et al. (2014)
Loess Region	1987–2016	0.69	0.59**	0.00	0.46**	0.75**	SWAT-DayCent	This study

Note: dashes mean the term is not applicable, ††means the nonlinear function with significant level of $P < 0.01$, *means the significant level of $P < 0.05$, **means the significant level of $P < 0.01$. The terms in Scott and Xiao indicate the relationships between Net Ecosystem Production (NEP) and climatic/hydrologic components. Pre indicates precipitation, Tem indicates temperature, SW indicates soil water, ET is the evapotranspiration.

4.4. Comparison of the current and globe-wide studies

In order to frame the study findings in a broader context, we compared our results with the globe-wide relationships between NPP and the climatic/hydrologic components (Table 3). Our results are well within the findings obtained with mechanism models and observations at different sites worldwide. In the arid/semi-arid regions, the central Asia and Inner Mongolia steppe grasses, the NPP exhibits significant positive relationship with precipitation but a moderate significant negative relationship with air temperature (Wang et al., 2014; Zhang and Ren, 2017). Our study area, UWRB, is semi-arid region, and we, not surprisingly, found that the NPP showed significant positive correlation with precipitation and almost no relationship with air temperature. Thus, in this sense, our study findings further strengthen the evidence that the vegetation production would be more sensitive to precipitation in such water-limited regions (Hsu et al., 2012). Differently, in high-elevation and cold regions, the Three-River Source Region (TRSR) and Tibetan Plateau, the NPP showed a relatively stronger positive relationship with air temperature compared to precipitation (Gao et al., 2013; Zhang et al., 2016b). High air temperature in the cold regions may accelerate the permafrost melt and lead to increment in soil water content indirectly, this then contributes to the vegetation growth to some extent (Gao et al., 2013). Because the soil water content plays a key role in determining the vegetation growth, especially in the arid/semi-arid region (Liu et al., 2013; Cleverly et al., 2016), and our study finding also fits rather well for this phenomenon. The model simulation, in-situ measurement, and flux observation at different sites worldwide also demonstrate that the ET and NPP are positively correlated, indicating the tightly coupled relationship between water and carbon cycles (Scott et al., 2014; Wang et al., 2014; Xiao et al., 2014; Scott et al., 2015). In this study, we also found that the carbon and water cycles were closely coupled in the semi-arid loess region using our newly-developed SWAT-DayCent model and the correlation coefficient between NPP and ET is somewhat larger than those in North America. This phenomenon may imply that the semi-arid loess region could use more water for sequestrating a given amount of carbon compared to others. Overall, these study results have important implications in terms of predictability of the vegetation growth and water loss in the semi-arid loess region. Nonetheless, we admitted that the model simulation should be applied to broader ranges and more varied climate conditions to verify these findings.

5. Implications

Climatic and hydrologic variability are among the primary controlling factors for terrestrial ecosystem production. Therefore, accurate prediction of their impacts on NPP would be valuable for decision making related to vegetation growth, food production, and the overall ecosystem management. This study indicates that the modeling approach, such as the one attempted here based on SWAT-DayCent coupler, can help quantify responses of ecosystem production to climatic and hydrologic variability at the regional scale, although we recognize that uncertainties do exist in the modeling results. Our spatial maps of the climatic controls can help policy makers identify the dominant climatic factor(s) over the local ecosystem production and develop appropriate adaptive strategies. The strong dependence of NPP on the water availability may also alert the watershed managers for such water-controlled basins to take more precautions for coping with the upcoming challenges of water resources scarcity. On the other hand, the climate warming, which is characterized by the increase in global mean temperature, has been regarded as an undoubted fact and could further exert adverse effects on the vegetation growth. In this sense, the watershed managers should also be aware of the impacts induced by climate warming, including droughts, through a scientific utilization and allocation of the water resource. For example, we suggest that the managers make more effective strategies, such as conservation tillage and improvement in irrigation system of the cropland, reasonable planning of cultivating season, scientific regulation of forest planting density, and reduction in the grazing intensity of the grassland, to improve the water-use efficiency in such regions.

Our modeling study also provided a proper perspective for investigating the main controlling environmental factors of the ecosystem production using a coupled model. This is certainly informative and valuable for people who are interested in the modeling research related to water and carbon cycles and their coupling process. For instance, the SWAT-DayCent coupler, employed in our study, can allow the users to simulate the hydrologic (e.g. streamflow) and biogeochemical processes (e.g. NPP) simultaneously and automatically. This can greatly facilitate the investigation of the water and carbon dynamics and their complex interactions. Therefore, it could be particularly beneficial to pay far more attention to approaches that involve coupling of models, especially when dealing with broader environmental issues and comprehensive assessments towards ensuring the sustainability of ecology, hydrology, economy, and society. In addition to the factors considered in the present study, the ecosystem production is also influenced by human intervention, such as the land use/land cover change. We will

examine the effects of anthropogenic influences in the future.

6. Limitations

It is essential to point out that only two representative climatic factors (precipitation and air temperature) and two hydrological factors (ET and soil water) were considered when investigating the control factors of NPP. It is true that other factors such as management practices and irrigated water supplies may also play important roles in the ecosystem production. Besides, the partial correlation analyses between NPP and the control factors were examined using a linear method, while the natural systems are quite complex and the responses may be nonlinear. Thus, multi-factorial analysis such as principal component analysis (PCA) might be a good method for future study.

7. Conclusions

In this study, we employed the SWAT-DayCent model to investigate the spatiotemporal change in NPP and its responses to climatic (precipitation and temperature) and hydrologic (soil water and evapotranspiration) factors. The SWAT-DayCent was proved to be an efficient tool for simulating the water and carbon cycles in the UWRB region. From 1987 to 2016, the regional NPP increased slightly but with no statistically significant trend. Spatially, the NPP exhibited a substantial variability over the region, with high NPP in the southeastern and western parts and low NPP in the northern part of the region. The correlation analysis showed that the precipitation was the main factor driving the ecosystem production and the average precipitation increase would have positive effects on NPP. However, the results also showed that higher temperature might exert negative effects on the production, especially in the southeastern part of the region. Furthermore, the NPP was positively correlated with the soil water and ET, indicating that the carbon gain relied heavily on the water availability and that the carbon and water cycles were tightly coupled in the loess region. Overall, the present study and the outcomes are useful for effective prediction of the response of terrestrial ecosystem carbon to the future climatic and hydrologic variability. The findings can also be helpful for making decisions related to ecosystem managements in such basins on the Loess Plateau, and even beyond.

Declaration of interest statement

The authors declare that they have no competing interests.

Acknowledgments

This study was funded by the National Thousand Youth Talent Program of China, Young Talent Support Plan of Xi'an Jiaotong University, National Natural Science Foundation of China (31741020), Postdoctoral Science Foundation of China (2016M592777), Natural Science Foundation of Guangdong Province (2016A050503035), and Innovation of Science and Technology Commission of Shenzhen (JCYJ20150521144320984). We also thank the HPCC Platform in Xi'an Jiaotong University for computing equipment and computer maintenance.

Appendix

A. Model performance evaluation

In order to assess model performance compared to observations, the following popular criteria were used in this study:

(I) Percentage bias (PB): It measures the average tendency of the simulated values to be larger or smaller than the observed ones, and is given by:

$$PB = \frac{1}{n}\sum_{i=1}^{n}\left(\frac{Q_{i,sim} - Q_{i,obs}}{Q_{i,obs}} \times 100\right) \quad (A.1)$$

where $Q_{i,obs}$ and $Q_{i,sim}$ are the observed and the simulated data, respectively; and n is the total number of data. The optimal value of PB is 0.0, with low-magnitude values indicating accurate model simulation, while positive or negative values indicate over-prediction or under-prediction of bias, respectively.

(II) Nash-Sutcliffe Efficiency (NSE) (Nash and Sutcliffe, 1970): It describes the explained variance for the observed values over time that is accounted for by the model. It is given by:

$$NSE = 1 - \frac{\sum_{i=1}^{n}(Q_{i,sim} - Q_{i,obs})^2}{\sum_{i=1}^{n}(Q_{i,obs} - \bar{Q}_{obs})^2} \quad (A.2)$$

The NSE ranges from a negative value to 1, and essentially, the closer to 1, the more accurate the model is.

(III) Correlation coefficient (r^2): It describes the proportion of the variance in the measured data explained by the model, or the linear relationship between the simulated and observed values. It is given by:

$$r^2 = \frac{\left(\sum_{i=1}^{n}(Q_{i,obs} - \bar{Q}_{obs})(Q_{i,sim} - \bar{Q}_{sim})\right)^2}{\sum_{i=1}^{n}(Q_{i,obs} - \bar{Q}_{obs})^2 \sum_{i=1}^{n}(Q_{i,sim} - \bar{Q}_{sim})^2} \quad (A.3)$$

where $\bar{Q}_{obs}$ and $\bar{Q}_{sim}$ are the mean values of the observed and the simulated runoff, respectively. An r^2 value nearer to 1.0 means that the model simulated highly accurately, whereas an r^2 value nearer to 0.0 means that the model simulated very poorly.

(IV) Root mean square error (RMSE): It measures the degree of deviation between measurements and model simulations.

$$\mathrm{RMSE} = \sqrt{\frac{\sum_{i=1}^{n}(Q_{i,sim} - Q_{i,obs})^2}{n}} \quad (A.4)$$

The RMSE varies from the optimal value to a large positive value, the lower the RMSE, the better the model performance.

B. Trend analysis

For trend analysis, the slope is calculated as follows:

$$\text{Slope} = \frac{n \times \sum_{i=1}^{n} i \times Var_i - \sum_{i=1}^{n} i \sum_{i=1}^{n} Var_i}{n \times \sum_{i=1}^{n} i^2 - (\sum_{i=1}^{n} i)^2} \quad \text{(B.1)}$$

where n represents the number of years and Var_i is the corresponding variable value. An increase of variables is only assumed if Slope $>$ 0, and a decrease of variables when Slope $<$ 0.

C. Correlation coefficient and partial correlation coefficient calculation

The Pearson correlation coefficient between two variables x and y is given by:

$$r_{xy} = \frac{\sum_{i=1}^{n} (x_i - \bar{x})(y_i - \bar{y})}{\sqrt{\sum_{i=1}^{n} (x_i - \bar{x})^2 \sum_{i=1}^{n} (y_i - \bar{y})^2}} \quad \text{(C.1)}$$

where x_i and y_i represent the time series of variable x (e.g. soil water) and variable y (e.g. NPP), respectively; and $\bar{x}$ and $\bar{y}$ are the average values of x and y.

The partial correlation coefficient between three variables x (e.g. precipitation), y (e.g. temperature), and z (e.g. NPP), is determined based on the Pearson correlation coefficient, and is given by:

$$r_{xy.z} = \frac{r_{xy} - r_{xz} r_{yz}}{\sqrt{(1 - r_{xy}^2)(1 - r_{yz}^2)}} \quad \text{(C.2)}$$

where $r_{xy.z}$ is the partial correlation coefficient, showing the relationship between variable x and variable y after excluding the effect variable z.

References

Arnold, J.G., Muttiah, R.S., Srinivasan, R., Allen, P.M., 2000. Regional estimation of base flow and groundwater recharge in the Upper Mississippi river basin. J. Hydrol. 227 (1–4), 21–40.

Arnold, J.G., Srinivasn, R., Muttiah, R.S., Willians, J.R., 1998. Large area hydrologic modeling and assessment – part I: model development. J. Am. Water Resour. As. 34 (1), 73–89.

Barkaoui, K., Navas, M.-L., Roumet, C., Cruz, P., Volaire, F., Power, S., 2017. Does water shortage generate water stress? An ecohydrological approach across Mediterranean plant communities. Funct. Ecol. 31 (6), 1325–1335.

Chen, C., Cleverly, J., Zhang, L., Yu, Q., Eamus, D., 2016. Modelling seasonal and inter-annual variations in carbon and water fluxes in an arid-zone acacia savanna woodland, 1981–2012. Ecosystems 19 (4), 625–644.

Ciais, P., Reichstein, M., Viovy, N., Granier, A., Ogee, J., Allard, V., et al., 2005. Europe-wide reduction in primary productivity caused by the heat and drought in 2003. Nature 437 (7058), 529–533.

Cleverly, J., Eamus, D., Coupe, N.R., Chen, C., Maes, W., Longhui, L., et al., 2016. Soil moisture controls on phenology and productivity in a semi-arid critical zone. Sci. Total Environ. 568, 1227–1237.

Del Grosso, S.J., Parton, W.J., Mosier, A.R., Walsh, M.K., Ojima, D.S., Thornton, P.E., 2006. DAYCENT national-scale simulations of nitrous oxide emissions from cropped soils in the United States. J. Environ. Qual. 35 (4), 1451–1460.

Feng, X., Fu, B., Lu, N., Zeng, Y., Wu, B., 2013. How ecological restoration alters ecosystem services: an analysis of carbon sequestration in China's Loess Plateau. Sci. Rep. 3, 2846.

Feng, X., Fu, B., Piao, S., Wang, S., Ciais, P., Zeng, Z., et al., 2016. Revegetation in China's Loess Plateau is approaching sustainable water resource limits. Nat. Clim. Change 6 (11), 1019–1022.

French, A.N., Hunsaker, D., Thorp, K., Clarke, T., 2009. Evapotranspiration over a cantelina crop at Maricopa, Arizona. Ind. Crops Prod. 29 (2–3), 289–300.

Fu, Z., Stoy, P.C., Luo, Y., Chen, J., Sun, J., Montagnani, L., et al., 2017. Climate controls over the net carbon uptake period and amplitude of net ecosystem production in temperate and boreal ecosystems. Agric. For. Meteorol. 243, 9–18.

Gao, Y., Zhou, X., Wang, Q., Wang, C., Zhan, Z., Chen, L., et al., 2013. Vegetation net primary productivity and its response to climate change during 2001–2008 in the Tibetan Plateau. Sci. Total Environ. 444, 356–362.

Gramig, B.M., Reeling, C.J., Cibin, R., Chaubey, I., 2013. Environmental and economic trade-offs in a watershed when using corn stover for bioenergy. Environ. Sci. Technol. 47 (4), 1784–1791.

Gu, F., Zhang, Y., Huang, M., Tao, B., Liu, Z., Hao, M., et al., 2017. Climate-driven uncertainties in modeling terrestrial ecosystem net primary productivity in China. Agric. For. Meteorol. 246, 123–132.

Hsu, J.S., Powell, J., Adler, P.B., 2012. Sensitivity of mean annual primary production to precipitation. Glob. Chang. Biol. 18 (7), 2246–2255.

Huang, X., Luo, G., Lv, N., 2017. Spatio-temporal patterns of grassland evapotranspiration and water use efficiency in arid areas. Ecol. Res. 32 (4), 523–535.

Jarvis, A., Reuter, H.I., Nelson, A., Guevara, E., 2006. Hole-filled seamless SRTM data VS. International Centre for Tropical Agriculture (CIAT), available from http://srtm.csi.cgiar.org.

Lauenroth, W.K., Wade, A.A., Williamson, M.A., Ross, B.E., Kumar, S., Cariveau, D.P., 2006. Uncertainty in calculations of net primary production for grasslands. Ecosystems 9 (5), 843–851.

Li, S., Lü, S., Zhang, Y., Liu, Y., Gao, Y., Ao, Y., 2014. The change of global terrestrial ecosystem net primary productivity (NPP) and its response to climate change in CMIP5. Theor. Appl. Clim. 121 (1–2), 319–335.

Liang, W., Yang, Y., Fan, D., Guan, H., Zhang, T., Long, D., et al., 2015. Analysis of spatial and temporal patterns of net primary production and their climate controls in China from 1982 to 2010. Agric. For. Meteorol. 204, 22–36.

Lima, J.R.d.S., Antonino, A.C.D., Souza, E.S.d., Lira, C.A.B.d.O., Silva, I.d.F.d., 2013. Seasonal and interannual variations of evapotranspiration, energy exchange, yield and water use efficiency of castor grown under rainfed conditions in northeastern Brazil. Ind. Crops Prod. 50, 203–211.

Liu, C., Dong, X., Liu, Y., 2015. Changes of NPP and their relationship to climate factors based on the transformation of different scales in Gansu, China. CATENA 125, 190–199.

Liu, D., Tian, F., Hu, H., Hu, H., 2012. The role of run-on for overland flow and the characteristics of runoff generation in the Loess Plateau, China. Hydrol. Sci. J. 57 (6), 1107–1117.

Liu, H., Tian, F., Hu, H.C., Hu, H.P., Sivapalan, M., 2013. Soil moisture controls on patterns of grass green-up in Inner Mongolia: an index based approach. Hydrol. Earth Syst. Sci. 17 (2), 805–815.

Lohse, K.A., Brooks, P.D., McIntosh, J.C., Meixner, T., Huxman, T.E., 2009. Interactions between biogeochemistry and hydrologic Systems. Annu. Rev. Environ. Resour. 34 (1), 65–96.

McCluney, K.E., Belnap, J., Collins, S.L., Gonzalez, A.L., Hagen, E.M., Nathaniel Holland, J., et al., 2012. Shifting species interactions in terrestrial dryland ecosystems under altered water availability and climate change. Biol. Rev. Camb. Philos. Soc. 87 (3), 563–582.

Moriasi, D.N., Arnold, J.G., Van Liew, M.W., Bingner, R.L., Harmel, R.D., Veith, T.L., 2007. Model evaluation guidelines for systematic quantification of accuracy in watershed simulations. Tran. ASABE 50 (3), 885–900.

Nash, J.E., Sutcliffe, J.V., 1970. River flow forecasting through conceptual models. Part i a discussion of principles. J. Hydrol. 10, 282–290.

Neitsch, S.L., Arnold, J.G., Kiniry, J.R., Willianms, J.R., 2011. Soil and Water Assessment Tool Theoretical Documentation Version 2009. Texas Water Resources Institute.

Noy-Meir, I., 1973. Desert ecosystems: environment and producers. Annu. Rev. Ecol. Syst. 4, 25–51.

Panagopoulos, Y., Gassman, P.W., Arritt, R.W., Herzmann, D.E., Campbell, T.D., Valcu, A., et al., 2015. Impacts of climate change on hydrology, water quality and crop productivity in the Ohio-Tennessee River Basin. Int. J. Agric. Biol. Eng. 8 (3), 36–53.

Parton, W.J., Hartman, M., Ojima, D., Schimel, D., 1998. DAYCENT and its land surface submodel: description and testing. Global Planet. Change 19, 35–48.

Parton, W.J., Ojima, D.S., Schimel, D.S., 1994. Environmental change in grasslands: assessment using models. Clim. Change 28 (1–2), 111–141.

Pei, F., Li, X., Liu, X., Lao, C., Xia, G., 2015. Exploring the response of net primary productivity variations to urban expansion and climate change: a scenario analysis for Guangdong Province in China. J. Environ. Manag. 150, 92–102.

Peng, H., Jia, Y., Niu, C., Gong, J., Hao, C., Gou, S., 2015. Eco-hydrological simulation of soil and water conservation in the Jinghe River Basin in the Loess Plateau, China. J. Hydro-environ. Res. 9 (3), 452–464.

Potter, C.S., Randerson, J.T., Field, C.B., Matson, P.A., Vitousek, P.M., Mooney, H.A., et al., 1993. Terrestrial ecosystem production: a process model based on global satellite and surface data. Global Biogeochem. Cycles 7 (4), 811–841.

Qiao, L., Zou, C.B., Will, R.E., Stebler, E., 2015. Calibration of SWAT model for woody plant encroachment using paired experimental watershed data. J. Hydrol. 523, 231–239.

Qiu, L., Hao, M., Wu, Y., 2017. Potential impacts of climate change on carbon dynamics in a rain-fed agro-ecosystem on the Loess Plateau of China. Sci. Total Environ. 577, 267–278.

Rafiqu, R., Kumar, S., Luo, Y., Kiely, G., Asrar, G., 2015. An algorithmic calibration

approach to identify globally optimal parameters for constraining the DayCent model. Ecol. Model. 297, 196–200.
Reyer, C.P., Leuzinger, S., Rammig, A., Wolf, A., Bartholomeus, R.P., Bonfante, A., et al., 2013. A plant's perspective of extremes: terrestrial plant responses to changing climatic variability. Glob. Chang. Biol. 19 (1), 75–89.
Running, S.W., Coughlan, J.C., 1988. A general model of forest ecosystem processes for regional applications I. Hydrologic balance, canopy gas exchange and primary production processes. Ecol. Model. 42, 125–154.
Scott, R.L., Biederman, J.A., Hamerlynck, E.P., Barron-Gafford, G.A., 2015. The carbon balance pivot point of southwestern U.S. semiarid ecosystems: Insights from the 21st century drought. J. Geophys. Res. Biogeosci. 120 (12), 2612–2624.
Scott, R.L., Huxman, T.E., Barron-Gafford, G.A., Darrel Jenerette, G., Young, J.M., Hamerlynck, E.P., 2014. When vegetation change alters ecosystem water availability. Glob. Chang. Biol. 20 (7), 2198–2210.
Su, C., Fu, B., 2013. Evolution of ecosystem services in the Chinese Loess Plateau under climatic and land use changes. Global Planet. Change 101, 119–128.
Sun, Y., Tian, F., Yang, L., Hu, H., 2014. Exploring the spatial variability of contributions from climate variation and change in catchment properties to streamflow decrease in a mesoscale basin by three different methods. J. Hydrol. 508, 170–180.
Tang, X., Li, H., Xu, X., Luo, J., Li, X., Ding, Z., et al., 2016. Potential of MODIS data to track the variability in ecosystem water-use efficiency of temperate deciduous forests. Ecol. Eng. 91, 381–391.
Vicente-Serrano, S.M., Camarero, J.J., Zabalza, J., Sangüesa-Barreda, G., López-Moreno, J.I., Tague, C.L., 2015. Evapotranspiration deficit controls net primary production and growth of silver fir: Implications for Circum-Mediterranean forests under forecasted warmer and drier conditions. Agric. For. Meteorol. 206, 45–54.
Wang, H., Sun, F., Xia, J., Liu, W., 2017a. Impact of LUCC on streamflow based on the SWAT model over the Wei River basin on the Loess Plateau in China. Hydrol. Earth Syst. Sci. 21 (4), 1929–1945.
Wang, P., Xie, D., Zhou, Y., Youhao, E., Zhu, Q., 2013. Estimation of net primary productivity using a process-based model in Gansu Province, Northwest China. Environ. Earth Sci. 71 (2), 647–658.
Wang, X., Li, F., Gao, R., Luo, Y., Liu, T., 2014. Predicted NPP spatiotemporal variations in a semiarid steppe watershed for historical and trending climates. J. Arid Environ. 104, 67–79.
Wang, X., Tan, K., Chen, B., Du, P., 2017b. Assessing the spatiotemporal variation and impact factors of net primary productivity in China. Sci. Rep. 7, 44415.
Wei, H., Fan, W., Ding, Z., Weng, B., Xing, K., Wang, X., et al., 2017. Ecosystem services and ecological restoration in the Northern Shaanxi Loess Plateau, China, in relation to climate fluctuation and investments in natural capital. Sustainability 9 (2), 199.
Wu, S., Zhou, S., Chen, D., Wei, Z., Dai, L., Li, X., 2014a. Determining the contributions of urbanisation and climate change to NPP variations over the last decade in the Yangtze River Delta, China. Sci. Total Environ. 472, 397–406.
Wu, Y., Liu, S., Abdul-Aziz, O.I., 2012. Hydrological effects of the increased CO_2 and climate change in the Upper Mississippi River Basin using a modified SWAT. Clim. Change 110, 977–1003.
Wu, Y., Liu, S., Huang, Z., Yan, W., 2014b. Parameter optimization, sensitivity, and uncertainty analysis of an ecosystem model at a forest flux tower site in the United States. J. Adv. Model. Earth Syst. 6 (2), 405–419.
Wu, Y., Liu, S., Li, Z., Dahal, D., Young, C.J., Schmidt, G.L., et al., 2014c. Development of a generic auto-calibration package for regional ecological modeling and application in the Central Plains of the United States. Ecol. Inform. 19, 35–46.
Wu, Y., Liu, S., Qiu, L., Sun, Y., 2016. SWAT-DayCent coupler: An integration tool for simultaneous hydro-biogeochemical modeling using SWAT and DayCent. Environ. Modell. Softw. 86, 81–90.
Wu, Y., Liu, S., Yan, W., 2014d. A universal Model-R Coupler to facilitate the use of R functions for model calibration and analysis. Environ. Modell. Softw. 62, 65–69.
Xiao, J., Ollinger, S.V., Frolking, S., Hurtt, G.C., Hollinger, D.Y., Davis, K.J., et al., 2014. Data-driven diagnostics of terrestrial carbon dynamics over North America. Agric. For. Meteorol. 197, 142–157.
Xin, Z., Yu, X., Li, Q., Lu, X.X., 2010. Spatiotemporal variation in rainfall erosivity on the Chinese Loess Plateau during the period 1956–2008. Reg. Environ. Change 11 (1), 149–159.
Xu, X., Yang, G., Tan, Y., Tang, X., Jiang, H., Sun, X., et al., 2017. Impacts of land use changes on net ecosystem production in the Taihu Lake Basin of China from 1985 to 2010. J. Geophys. Res. Biogeosci. 122 (3), 690–707.
Yan, R., Zhang, X., Yan, S., Zhang, J., Cheng, H., 2017. Spatial patterns of hydrological responses to land use/cover change in a catchment on the Loess Plateau, China. Ecol. Indic. 92, 151–160.
Zhang, C., Ren, W., 2017. Complex climatic and CO_2 controls on net primary productivity of temperate dryland ecosystems over central Asia during 1980–2014. J. Geophys. Res. Biogeosci. 122, 2356–2374.
Zhang, S., Yang, D., Yang, Y., Piao, S., Yang, H., Lei, H., et al., 2018. Excessive afforestation and soil drying on China's Loess Plateau. J. Geophys. Res. Biogeosci. 123 (3), 923–935.
Zhang, T., Peng, J., Liang, W., Yang, Y., Liu, Y., 2016a. Spatial-temporal patterns of water use efficiency and climate controls in China's Loess Plateau during 2000–2010. Sci. Total Environ. 565, 105–122.
Zhang, Y., Song, C., Zhang, K., Cheng, X., Band, L.E., Zhang, Q., 2014. Effects of land use/land cover and climate changes on terrestrial net primary productivity in the Yangtze River Basin, China, from 2001 to 2010. J. Geophys. Res. Biogeosci. 119 (6), 1092–1109.
Zhang, Y., Zhang, C., Wang, Z., Chen, Y., Gang, C., An, R., et al., 2016b. Vegetation dynamics and its driving forces from climate change and human activities in the Three-River Source Region, China from 1982 to 2012. Sci. Total Environ. 563–564, 210–220.
Zhao, A., Zhu, X., Liu, X., Pan, Y., Zuo, D., 2016. Impacts of land use change and climate variability on green and blue water resources in the Weihe River Basin of northwest China. CATENA 137, 318–327.
Zhao, F., Wu, Y., Qiu, L., Bellie, S., Zhang, F., Sun, Y., et al., 2018a. Spatiotemporal features of the hydro-biogeochemical cycles in a typical loess gully watershed. Ecol. Indic. 91, 542–554.
Zhao, F., Wu, Y., Qiu, L., Sun, Y., Sun, L., Li, Q., et al., 2018b. Parameter uncertainty analysis of the SWAT model in a mountain-loess transitional watershed on the Chinese Loess Plateau. WATER 10 (6), 690.
Zhao, M., Heinsch, F.A., Nemani, R.R., Running, S.W., 2005. Improvements of the MODIS terrestrial gross and net primary production global data set. Remote Sens. Environ. 95 (2), 164–176.
Zhao, M., Running, S.W., Nemani, R.R., 2006. Sensitivity of Moderate Resolution Imaging Spectroradiometer (MODIS) terrestrial primary production to the accuracy of meteorological reanalyses. J. Geophys. Res. 111 (G1).
Zhou, G., Wei, X., Wu, Y., Liu, S., Huang, Y., Yan, J., et al., 2011. Quantifying the hydrological responses to climate change in an intact forested small watershed in Southern China. Glob. Chang. Biol. 17 (12), 3736–3746.
Zuo, D., Xu, Z., Wu, W., Zhao, J., Zhao, F., 2014. Identification of streamflow response to climate change and human activities in the Wei River Basin, China. Water Resour. Manag. 28 (3), 833–851.